

## Doping of charge density wave in $\text{Ba}_{1-x}\text{K}_x\text{BiO}_3$

J. Yu, X. Y. Chen, and W. P. Su

*Department of Physics and Texas Center for Superconductivity, University of Houston, Houston, Texas 77204-5504*

(Received 16 June 1989)

We study the formation of charge density waves (CDW) in  $\text{Ba}_{1-x}\text{K}_x\text{BiO}_3$  within a tight-binding model proposed by Prelovsek, Rice, and Zhang. Light doping leads to the formation of immobile bipolarons. The charge density wave amplitude diminishes gradually as doping concentration increases and disappears at about 35% doping. We have calculated the density of states and optical properties for various doping concentrations. We also present corresponding results in two dimensions that are applicable to a CDW system with the  $\text{La}_2\text{CuO}_4$  geometry.

### I. INTRODUCTION

The discovery of the new copper-free high- $T_c$  compound<sup>1,2</sup>  $\text{Ba}_{1-x}\text{K}_x\text{BiO}_3$  provides a very interesting contrast to the copper oxides.<sup>3,4</sup> There is evidence that antiferromagnetism is linked to superconductivity in the cuprates.<sup>5,6</sup> It is therefore natural to speculate that CDW is related to superconductivity in potassium compounds.<sup>7,8</sup>

In this paper we undertake a mean-field-theory study of the CDW formation utilizing a model proposed by Prelovsek, Rice, and Zhang (PRZ).<sup>9</sup> The Hamiltonian is introduced in Sec. II. We first solve the model in two dimensions numerically for various doping levels. Inhomogeneous solutions are found in the lightly doped case corresponding to the formation of polarons and bipolarons. These localized objects are pinned by the discrete lattice for realistic parameter values. As the doping increases the bipolarons merge into domains of CDW with alternate signs. The average CDW amplitude varies smoothly with doping concentration as it would be in a homogeneous solution. After a critical concentration is reached, the charge density wave disappears completely. The two-dimensional results are presented in Sec. III.

The results in three dimensions (Sec. IV) are similar. The bipolarons are pinned. There is a critical concentration for the CDW to exist. As doping progresses the electronic gap is gradually reduced. It disappears before the critical composition is reached.

To monitor the electronic properties we have calculated the optical absorption spectrum corresponding to various doping concentrations. Comparison with existing data on  $\text{Ba}_{1-x}\text{K}_x\text{BiO}_3$  will be made. Finally we briefly discuss possible relevance of CDW to superconductivity in Sec. V.

### II. MODEL HAMILTONIAN

Following PRZ we first consider a square  $\text{CuO}_2$  lattice with one electron state per Cu. By assuming a deformation-potential-type interaction between the electron and the breathing mode of O atoms, one obtains the following Hamiltonian:

$$H = -t \sum_{\langle i,j \rangle, s} (c_{i,s}^\dagger c_{j,s} + \text{H.c.}) - 4V \sum_{i,s} \bar{u}_i c_{i,s}^\dagger c_{i,s} + \frac{K}{2} \sum_i (x_i^2 + y_i^2) + \frac{M}{2} \sum_i (\dot{x}_i^2 + \dot{y}_i^2), \quad (1a)$$

$$\bar{u}_i = \frac{1}{4}(x_{i_x, i_y} - x_{i_x-1, i_y} + y_{i_x, i_y} - y_{i_x, i_y-1}), \quad (1b)$$

where  $x_i, y_i$  denote displacements of both O atoms in the unit cell, and  $i = (i_x, i_y)$ . For later applications it is useful to regard the local single-electron state as a Wannier state consisting of the antibonding combination of the Cu orbital and the four surrounding oxygen orbitals.

To solve the model in the adiabatic approximation, we numerically iterate the Hartree equations corresponding to Hamiltonian (1). Periodic boundary conditions are used.

As it stands there are three parameters  $t$ ,  $V$ , and  $K$  in the Hamiltonian (1). By rescaling the oxygen displacements one parameter can be eliminated.

### III. TWO-DIMENSIONAL CDW

For the two-dimensional calculations, we set  $t = 1$  corresponding to a bandwidth of 8. The coupling constant is so chosen that the energy gap  $E_g$  at half filling ( $\rho = \frac{1}{2}$ ) is 3.0.

To see the effect of doping on the CDW we plot the staggered displacement

$$\phi_{i_x, i_y} = \bar{u}_{i_x, i_y} (-1)^{i_x + i_y} \quad (2)$$

in Fig. 1 for various filling fractions  $\rho$ . The size of the lattice is  $10 \times 10$ . For  $\rho = \frac{1}{2}$  there are 100 electrons. By taking out one electron, a localized polaron solution is formed. For two holes the minimum energy configuration is a bipolaron [Fig. 1(a)]. There seems to be a tendency for the bipolarons to cluster as seen in the 6-, 14-, and 16-hole configurations [Figs. 1(b)–(1d)]. At 20% and 24% doping [Fig. 1(e) and 1(f)], the normalized order parameter actually becomes  $-1.0$ , i.e., a half of the system is close to one of the degenerate ground states at

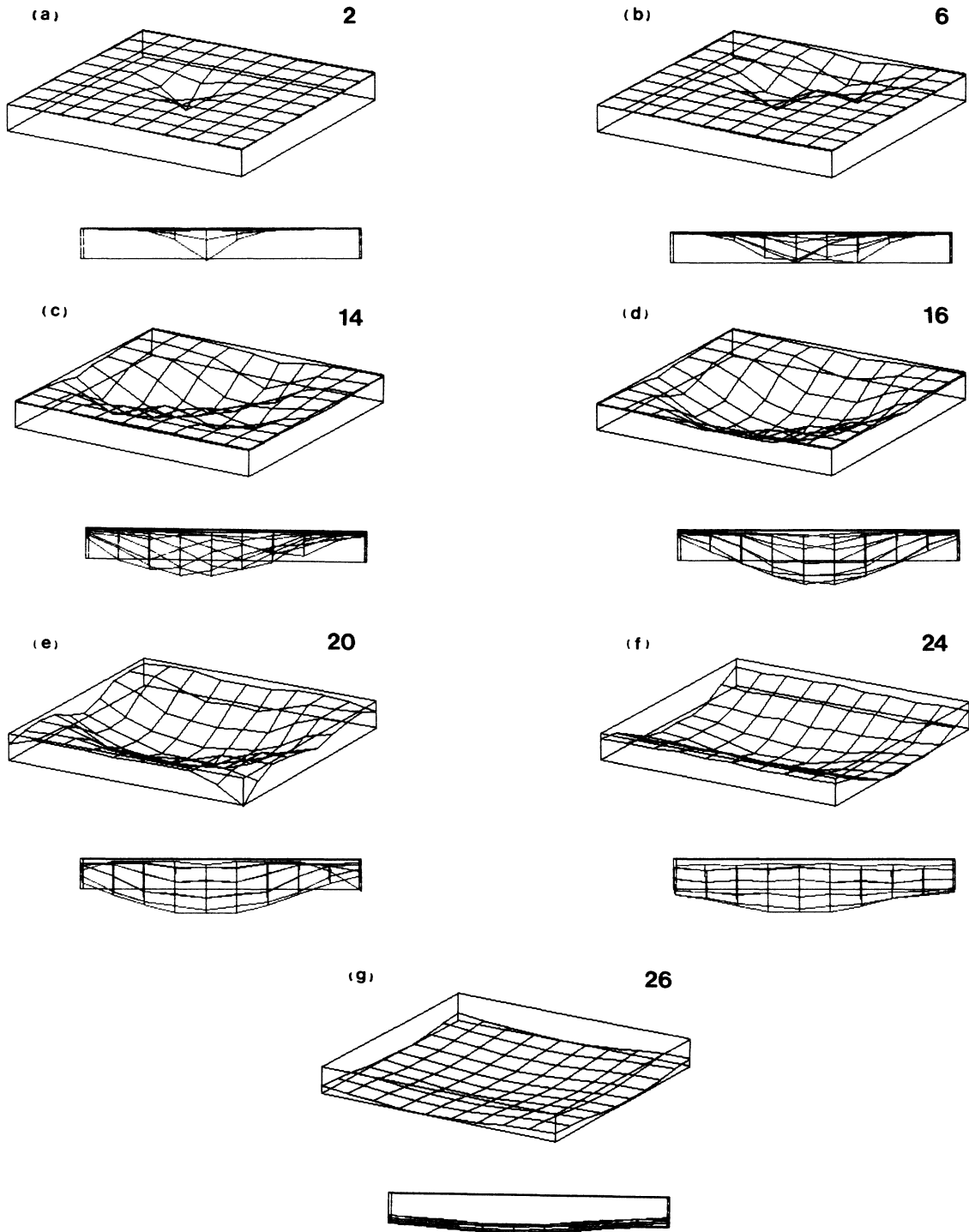


FIG. 1. Perspective view and side view of the lattice configurations in terms of the normalized staggered displacement (2) for various numbers of holes  $n$  on a  $10 \times 10$  lattice.

$\rho = \frac{1}{2}$ , whereas the other half is closer to the other ground state. The average staggered order parameter is very small. At an even higher doping level the CDW is almost entirely gone.

Figure 2 shows the density of states for various numbers of holes. The arrow indicates the position of the Fermi energy. Associated with each bipolaron there is a

gap state that is unoccupied. The electronic gap is gradually reduced as doping progresses. It vanishes before CDW is completely gone. We should point out that in general for each  $\rho$  there exist many inhomogeneous solutions with about the same energy. They are not related by translation. The qualitative features are, however, about the same.

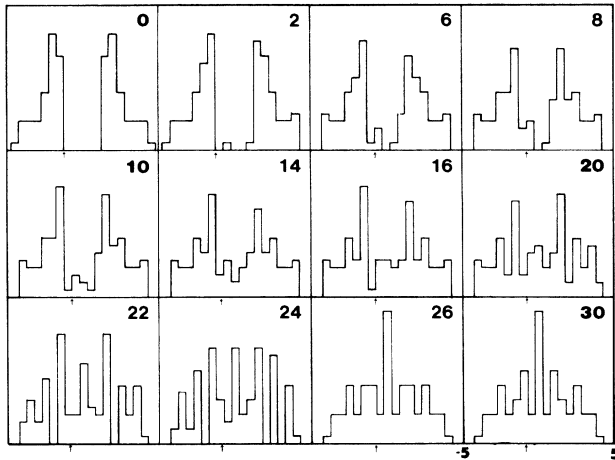


FIG. 2. Density of states corresponding to various number of holes on a  $10 \times 10$  lattice. The arrow indicates the position of the Fermi energy.

In the lightly doped systems polarons and bipolarons are the elementary excitations.<sup>10</sup> It is of central interest to study their individual properties and their interactions. In this context the first thing to note is that we are dealing with a discrete lattice so both polarons and bipolarons require some activation energy to move continuously from one site to another. We estimate the activation energy by rigidly shifting the polaron or bipolaron profile continuously and calculate the total energy for each lattice configuration. The result is shown in Fig. 3 for several values of the energy gap. The activation energy for a bipolaron (the upper curve) is much larger than that of a polaron, and both activation energies could be a substantial fraction of the energy gap  $E_g$ . For example, with  $E_g = 1.5$  eV the bipolarons are practically pinned at room temperature.

Turning now to the interaction, Fig. 4(a) shows the potential energy between two polarons as a function of their distance. In calculating the potential energy one polaron is placed at the origin, while the other polaron is dis-

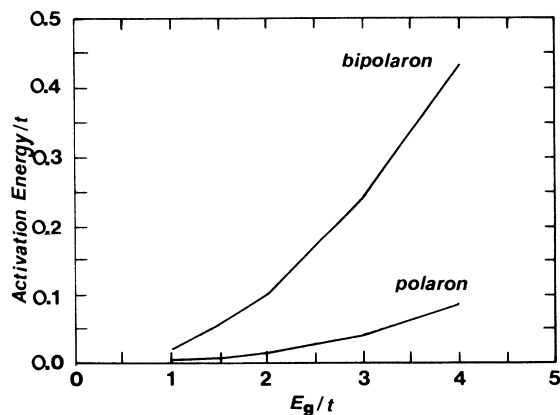


FIG. 3. Activation energy for the motion of a bipolaron or a polaron on a two-dimensional lattice vs energy gap.

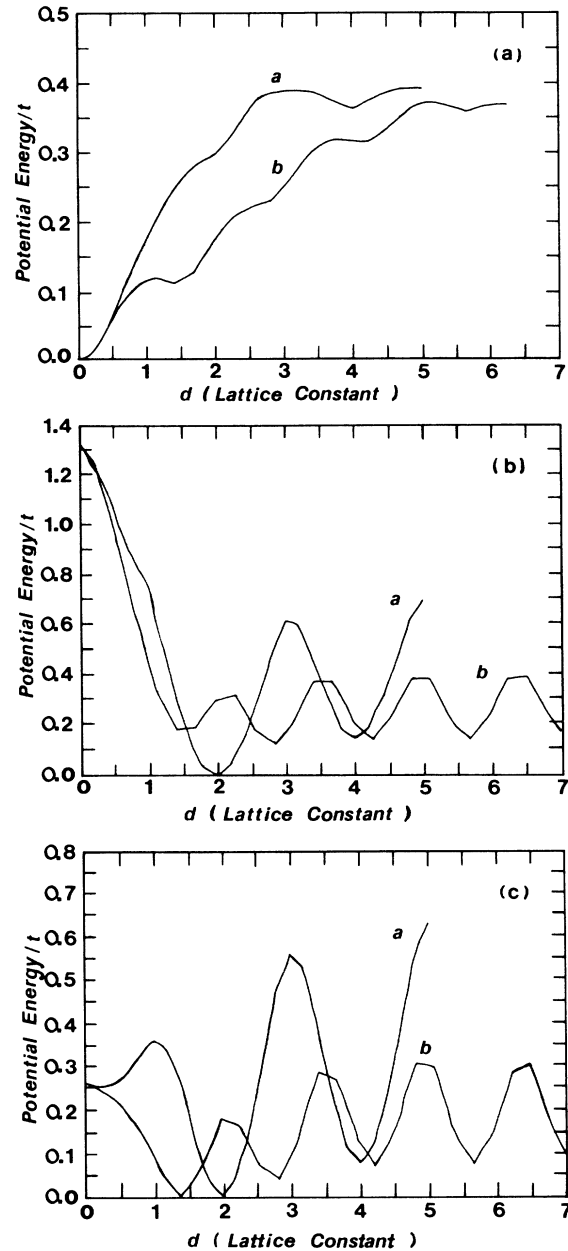


FIG. 4. Potential energy between (a) two polarons, (b) two bipolarons, and (c) a polaron and a bipolaron plotted as function of the separation between the two objects. (The curve *a* refers to a separation in the [10] direction, *b* in the [11] direction.)

placed in a diagonal direction. There is a strong attractive interaction. The potential energy reaches a maximum at about  $d = 5$  because of the finite-size effect. The lattice pinning energy is also clear from the potential energy curve. Similarly, Fig. 4(c) depicts the interaction between a polaron and a bipolaron. Figure 4(b) is for two bipolarons. There is a relatively weak attraction between the bipolarons.

Optical absorption provides another way to monitor the change induced by doping. Figure 5 shows the optical density for various numbers of holes. Note that even

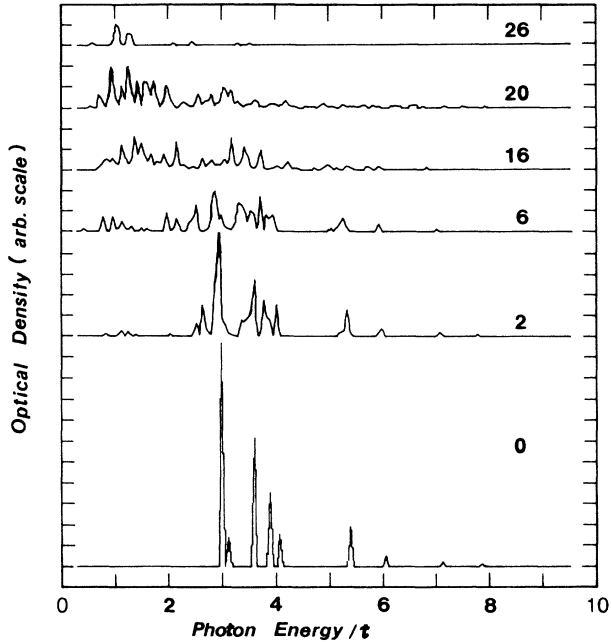


FIG. 5. Optical density for various number of holes on a  $10 \times 10$  lattice.

at 6% doping there is a substantial absorption within the gap.

To end this section we present the CDW pattern viewed in perspective for various doping levels in Fig. 6. The sawtooth background represents a uniform charge

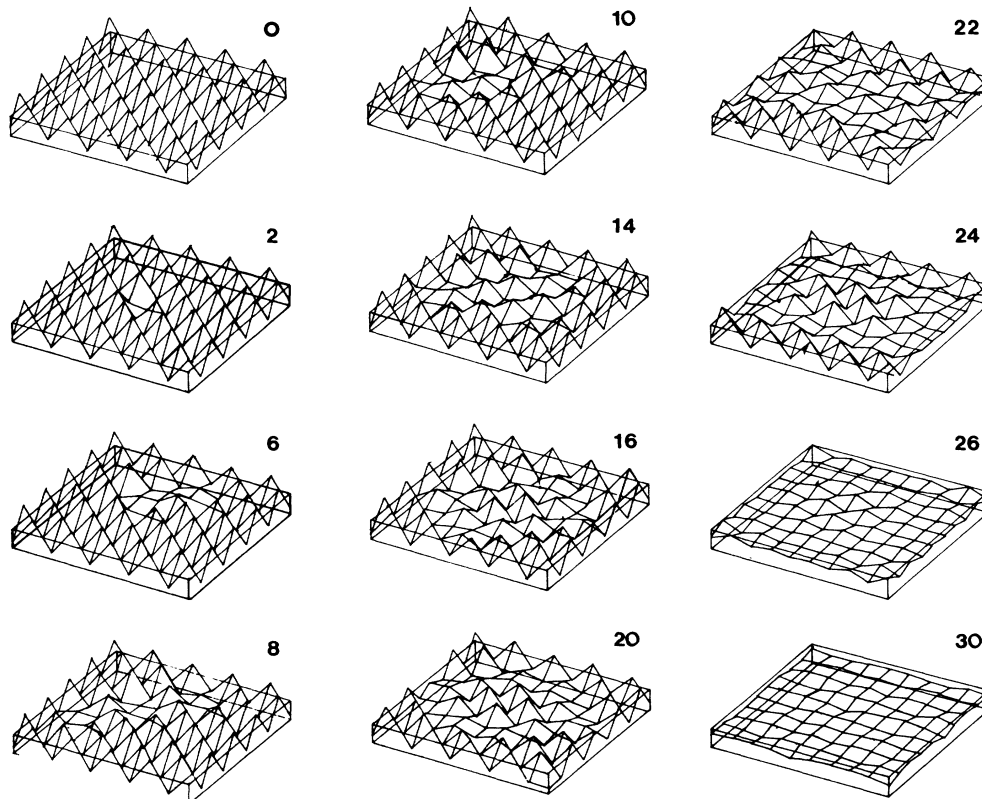


FIG. 6. Perspective view of CDW pattern corresponding to various number of holes on a  $10 \times 10$  lattice.

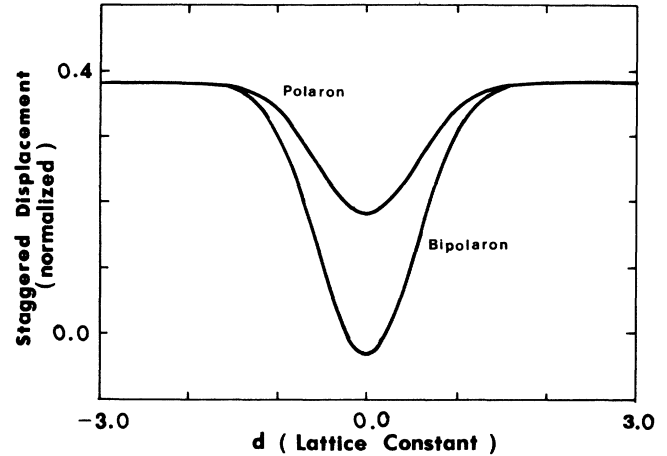


FIG. 7. Profiles of a polaron and a bipolaron. The staggered order parameter is plotted as a function of the radial distance  $r$ .

disproportion. Doping leads to the disruption of charge disproportion and eventually destroys it.

#### IV. THREE-DIMENSIONAL CDW

To discuss the CDW in  $Ba_{1-x}K_xBiO_3$  we simply generalize the two-dimensional  $CuO_2$  geometry to the three-dimensional  $BiO_3$  geometry. Unlike the two-dimensional case it is not easy to present the results in graphs. We have to rely more on verbal descriptions.

For the three-dimensional calculations we have primarily taken the gap to be  $E_g = 4$ , which is about a quarter of the bandwidth. This ratio is about the same as that inferred from the optical data on  $\text{BaBiO}_3$  by Tajima *et al.*<sup>11-13</sup> The calculations are done on a  $6 \times 6 \times 6$  lattice with periodic boundary conditions.

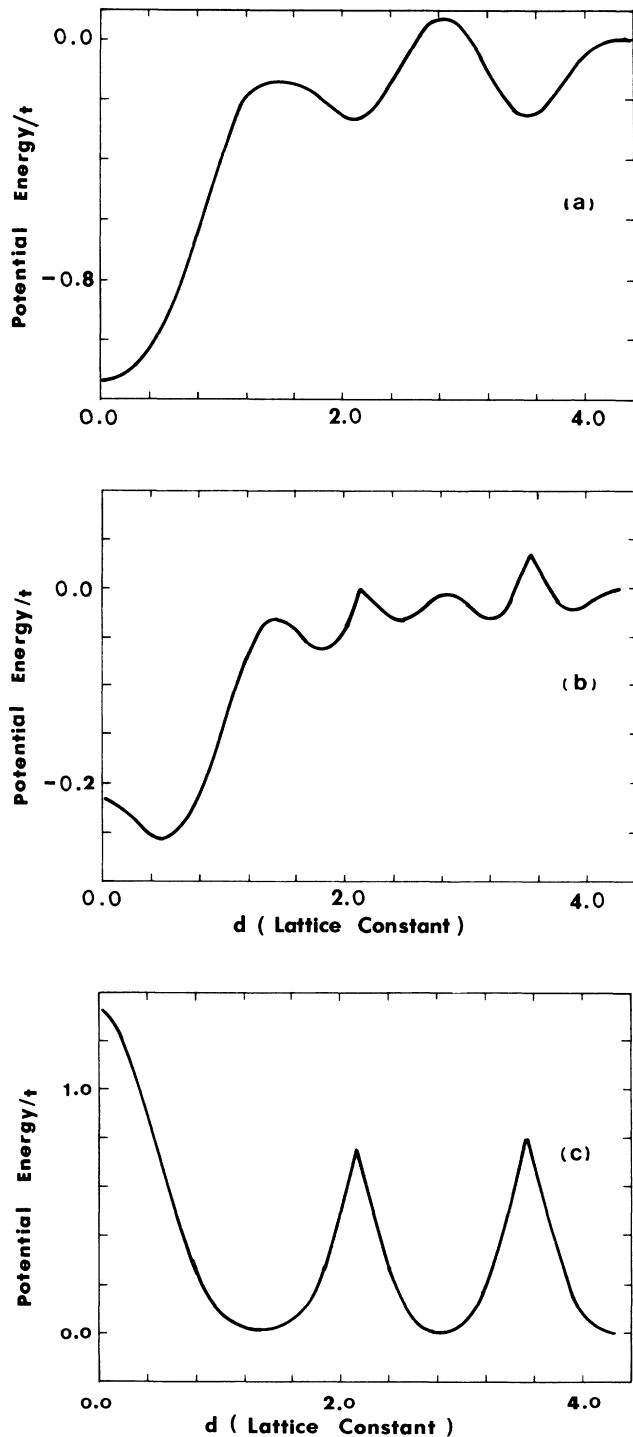


FIG. 8. Potential energy between (a) two polarons, (b) a polaron and a bipolaron, and (c) two bipolarons plotted as function of the separation between the two objects in the [110] direction.

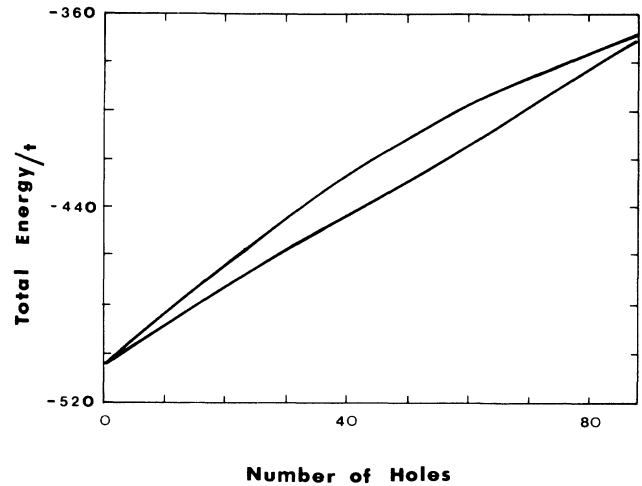


FIG. 9. Total energy of the homogeneous solution (upper curve) and the inhomogeneous solution (lower curve) as a function of the number of holes on a  $6 \times 6 \times 6$  lattice.

Just as in two dimensions, light doping leads to formation of polarons and bipolarons. The size of a polaron or a bipolaron is very small as shown in Fig. 7. Essentially it is a depression of the order parameter on a single site. For that reason the activation energy for the motion of a bipolaron is very large as can be seen from the potential energy curve for a pair of bipolarons [Fig. 8(c)]. The strong binding energy of a bipolaron is depicted in Fig. 8(a). Figure 8(b) shows that there is a hard-core repulsion between a polaron and a bipolaron. The same goes between two bipolarons.

As doping proceeds, clusters or domains are formed. At around 30% doping, which is a critical concentration for an uniform CDW to exist, domains with both positive and negative staggered order parameters are present. This type of fluctuations persists to 40% doping, beyond which the lattice is completely undistorted. The difference between a homogeneous solution and an inhomogeneous solution is also shown in Fig. 9 in terms of the total ground state energy.

The change in the density of states induced by doping is qualitatively the same as the two-dimensional case. Gap states appear and substantially perturb the gap structure long before CDW is destroyed (Fig. 10). This effect is also reflected in the absorption spectrum (Fig. 11). The significant subgap absorption at a low doping level is a key signature of polaronic objects.<sup>10</sup> Such a feature is not found in the optical data<sup>11-13</sup> on  $\text{Ba}_{1-x}\text{Pb}_x\text{BiO}_3$  and  $\text{Ba}_{1-x}\text{K}_x\text{BiO}_3$ . A more sophisticated model is probably needed to fully explain the observed absorption spectra.

We conclude this section by mentioning that we have tried to calculate the effective mass of a bipolaron by estimating the kinetic energy of the atoms associated with the motion of a bipolaron. Due to the strong localized nature of the bipolaron, the effective mass depends on where the center of a bipolaron is. For a bipolaron centered on a lattice site, the effective mass is comparable to

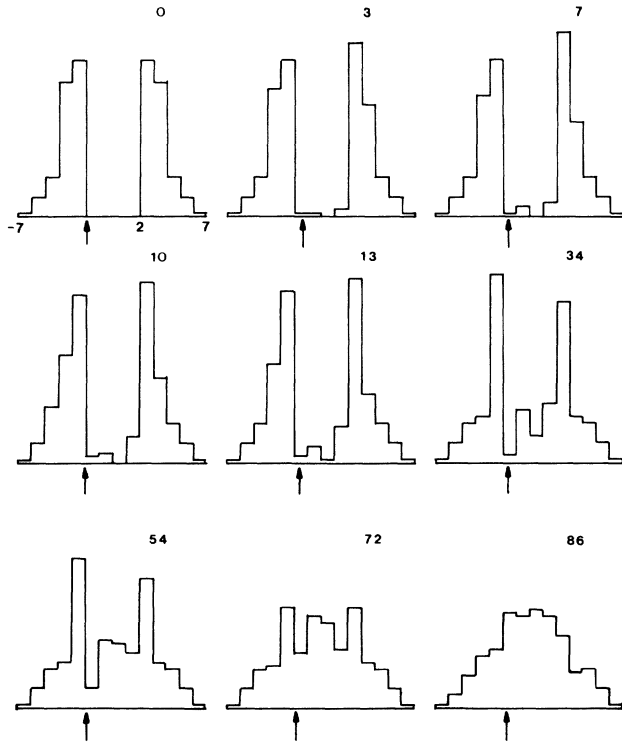


FIG. 10. Density of states corresponding to various doping concentrations on a  $6 \times 6 \times 6$  lattice. The arrow indicates the position of the Fermi energy.

the oxygen atomic mass. From that we have found that the quantum lattice effect is negligible.

## V. DISCUSSION

It is clear from the preceding sections that a bipolaron Bose-Einstein condensation is unlikely. We must therefore consider other explanations for the observed high  $T_c$ . Machida<sup>14</sup> has proposed a density-of-states enhancement mechanism. He argues that a preexisting CDW with the gap edge singularity helps to increase the density of the states at the Fermi level and therefore enhances  $T_c$ . For his argument he assumes a uniform CDW. As we see from both Figs. 2 and 10, in an inhomogeneous CDW the density of states at the Fermi energy is not singular. On the contrary it is likely to be smaller than that of an undistorted lattice. So we do not think his argument holds. Besides, the optimal  $T_c$  is found at a composition in which there is no long-range CDW order.<sup>15</sup>

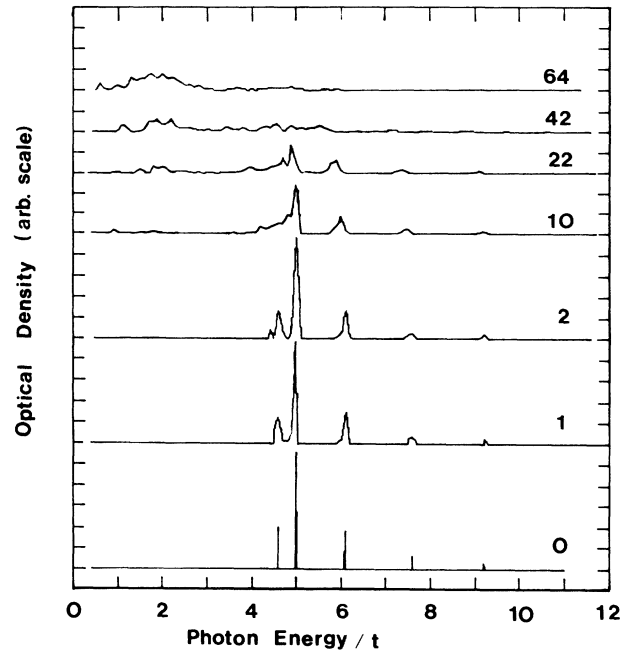


FIG. 11. Optical density for various number of holes on a  $6 \times 6 \times 6$  lattice.

In the absence of a quantitative calculation of the superconducting properties of the model, some speculation is not completely out of order. As we have seen, near the metal-insulator transition the CDW is weak and the domains are quite extended. In such a CDW background the charge carriers should be mobile. With some CDW fluctuations around, certain attractive interactions between the mobile carriers could still be induced. In other words we favor a picture in which the  $T_c$  is enhanced by residual CDW fluctuations that can exist only in an inhomogeneous solution.

## ACKNOWLEDGMENTS

We thank Dr. Barry Friedman and Dr. Gregory Levine for useful discussions. This work was supported by the Robert A. Welch Foundation, the Texas Advanced Research Program under Grant No. 1053, and by the Texas Center for Superconductivity at the University of Houston under prime Grant No. MDA 972-88-6-0002 to the University of Houston from Defense Advanced Research Projects Agency and the State of Texas.

<sup>1</sup>R. J. Cava *et al.*, Nature **322**, 814 (1988).

<sup>2</sup>D. G. Hinks *et al.*, Nature **333**, 836 (1988).

<sup>3</sup>J. G. Bednorz and K. A. Müller, Z. Phys. B **64**, 189 (1986).

<sup>4</sup>M. K. Wu *et al.*, Phys. Rev. Lett. **58**, 908 (1987).

<sup>5</sup>J. R. Schrieffer, X. G. Wen, and S. C. Zhang, Phys. Rev. Lett. **60**, 944 (1988).

<sup>6</sup>W. P. Su and X. Y. Chen, Phys. Rev. B **38**, 8879 (1988).

<sup>7</sup>T. M. Rice, Nature **332**, 780 (1988).

<sup>8</sup>J. R. Schrieffer, X. G. Wen, and S. C. Zhang, Mod. Phys. Lett. B **2**, 935 (1988).

<sup>9</sup>P. Prelovsek, T. M. Rice, and F. C. Zhang, J. Phys. C **20**, L229 (1987).

<sup>10</sup>A. J. Heeger, S. Kivelson, J. R. Schrieffer, and W. P. Su, Rev. Mod. Phys. **60**, 781 (1988).

<sup>11</sup>S. Tajima *et al.*, Phys. Rev. B **32**, 6302 (1985).

<sup>12</sup>S. Tajima *et al.*, Phys. Rev. B **35**, 696 (1987).

<sup>13</sup>H. Sato, S. Tajima, H. Takagi, and S. Uchida, Nature **338**, 241 (1989).

<sup>14</sup>K. Machida, Physica C **156**, 276 (1988).

<sup>15</sup>L. F. Schneemeyer *et al.*, Nature **335**, 421 (1988).